Journal of Materials Chemistry A

ROYAL SOCIETY OF CHEMISTRY

PAPER

View Article Online
View Journal | View Issue

Cite this: J. Mater. Chem. A, 2024, 12, 17501

Sandwiching high energy frameworks by taking advantage of π-philic molecular recognition†

Jatinder Singh, [a] Richard J. Staples, [b] Magdalena Fabin [ac] and Jean'ne M. Shreeve *[a]

Development of thermally stable, insensitive materials with attractive physiochemical properties continues to be heavily pursued in the field of energetic materials. High-energy-density compounds assembled by the combination of polynitro, nitroamino or azo groups and nitrogen-rich frameworks are often thermally unstable and sensitive to impact and friction. This conflicting nature of energy and stability strongly encourages designers of molecules to study existing structures at the molecular level in order to develop new methodologies for construction of potential energetic materials. In this work, a robust strategy which takes advantage of π-philic molecular recognition between planar energetic anions and cations is pursued. Our work not only generates insights for the design and synthesis of new energetic sandwich salts with good thermal stability and low sensitivity but also inspires the enrichment of a variety of new excellent performing high-energy materials.

Received 11th April 2024
Accepted 12th June 2024

DOI: 10.1039/d4ta02521k

rsc.li/materials-a

1 Introduction

Noncovalent attractions are associations within and between molecules that influence shape and structural stability.[1,2] Nearly all organic materials involve these attractions, which influence physical and chemical properties markedly.[3,4] π-Philic molecular recognition between planar aromatic organic rings (often known as weak π–π interactions) play an important role in the field of chemistry and biology.[5] These attractions have also been the subject of extensive computational and experimental studies since they play a complex function prior to or at the transition state in chemical reactions and catalytic processes; for example, they are central to understanding the stability of DNA, protein folding and drug binding.[6] Molecular recognition between π-systems of planar aromatic organic rings often leads to the formation of stacked structures (Fig. 1B).[7] In supramolecular chemistry, π-philic molecular recognition offers potential opportunities for tailoring structure and properties to various functions and applications (Fig. 1C).[8,9] Recently, supramolecules as π-philic molecular sensors were applied in the detection of nitroaromatics.[10] Among energetic materials, 1,3,5-triamino 2,4,6-trinitrobenzene (TATB) is a well-known highly stable compound owing to the synergetic effect of various noncovalent attractions such as inter/intra-molecular H-bond and π-stacking (Fig. 1E). A better understanding of weak attractions would be helpful in crystal engineering, molecular recognition, and in the design of future energetic materials.[11–14]

Energetic salt formation is an efficient strategy to maximize weak noncovalent interactions.[15–20] Energetic salts also generate a single multifunctional product efficiently by incorporating two or more reactants and thus is regarded as a highly useful strategy to expand molecular diversity and complexity.[21] This simple conventional methodology also showcases the art of holding two or more units together by weak interactions and is regarded as the most useful in producing thermally stable energetic materials. For instance, dihydroxylammonium 5,5′-bistetrazole-1,1′-diolate (TKX-50) possesses higher thermal stability and better detonation performance than its precursors (Fig. 2A), suggesting that salt formation is an effective method to access stable energetic materials.[22–25]

Despite the effectiveness of salt formation strategy, energetic salts produced from N-rich cations and sensitive anions are often unable to overcome their inherent sensitivity to external stimuli.[26–28] One other unresolved issue in the development of energetic salts is their high solubility in water, which raises concerns and difficulties associated with their use.[29,30] Therefore, it is important for synthetic and theoretical researchers to resolve these issues by developing new methods. Now designers of molecules have turned their attention increasingly to the development of approaches to maximize the stabilizing interaction by producing

[a]Department of Chemistry, University of Idaho, Moscow, Idaho, 83844-2343, USA. E-mail: jshreeve@uidaho.edu; Fax: (+1) 208-885-5173

[b]Department of Chemistry, Michigan State University, East Lansing, Michigan, 48824, USA

[c]Department of Physical Chemistry and Technology of Polymers, Silesian University of Technology, 44-100 Gliwice, Poland

† Electronic supplementary information (ESI) available: Synthesis of compounds, isodesmic reactions, characterization data. CCDC 2100988 (**ISEM-1**); 2345095 (**ISEM-2**); 2345096 (**ISEM-3**); 2345097 (**ISEM-4**); 2345098 (**ISEM-5**); 2345099 (**9-TATOT**); 2346398 (**ISEM-3-H_2O**); 2350606 (**ISEM-6**); 2350679 (**ISEM-6-H_2O**). For ESI and crystallographic data in CIF or other electronic format see DOI: https://doi.org/10.1039/d4ta02521k

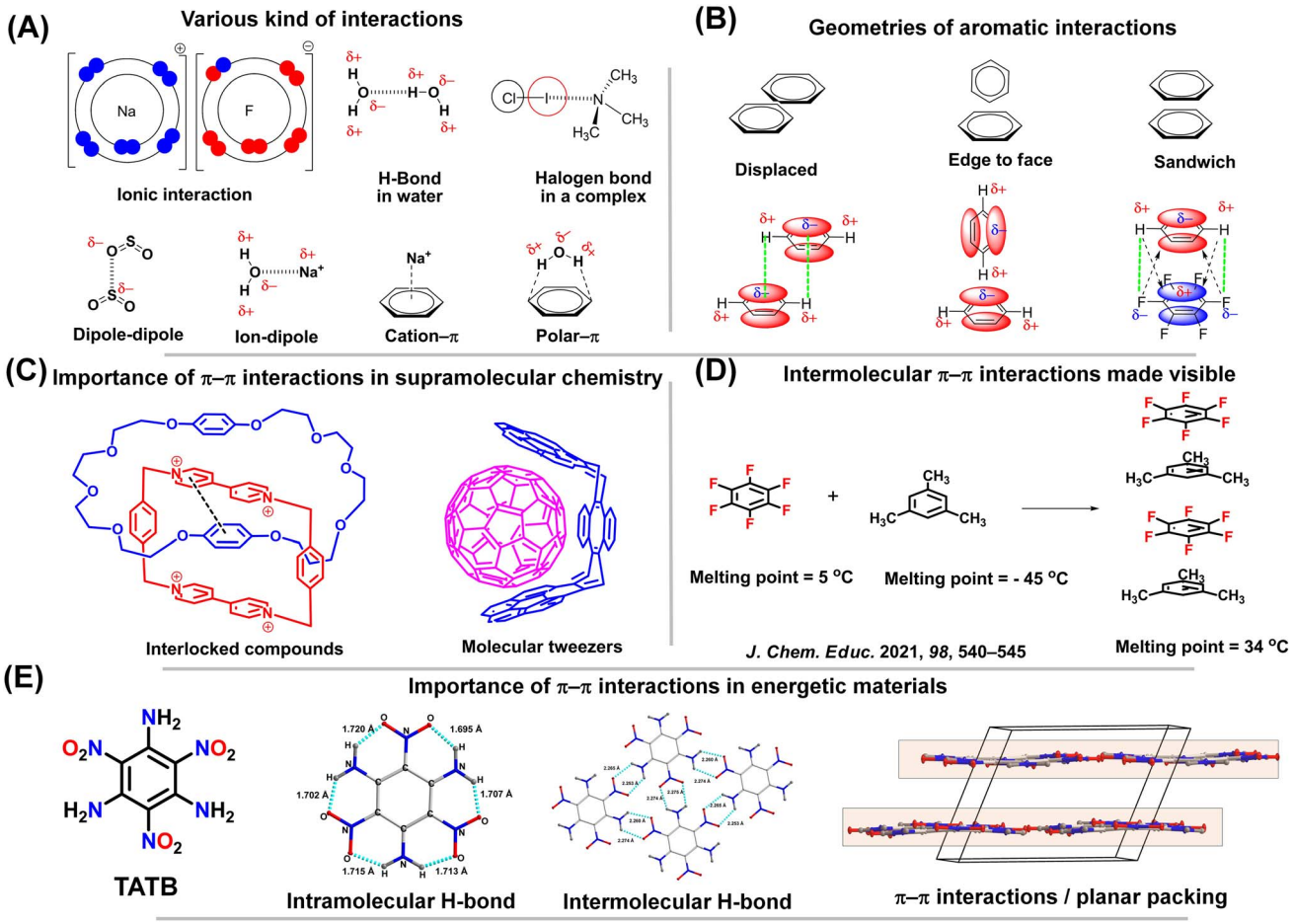

Fig. 1 (A–E) Noncovalent interactions and their applications in various fields.

planar energetic metal–organic frameworks, hydrogen-bonded organic frameworks, polymers, co-crystals, *etc.* (Fig. 2B–D).[31–35]

In all the above techniques, weak attractions play a central role in overcoming the issues related to thermal stability, sensitivity, acidity and solubility in water. In 2015, Klapötke and coworkers demonstrated the utility of a planar 3,6,7-triamino-7*H*-[1,2,4]triazolo[4,3-b][1,2,4]triazolium (TATOT) cation in making thermally stable energetic nitrogen-rich cationic salts.[36] Recently, we reported that salt formation between a planar dinitramide and TATOT results in better thermal stability and insensitivity in comparison to other N-rich salts.[37] Now we have analyzed the structure at the molecular level and extended the observation to other thermally unstable and sensitive frameworks. We anticipated that salt formation between similar planar frameworks and TATOT could lead to π-philic molecular recognition and sandwich type structures, which would be useful in stabilizing high-energy-high-sensitive compounds. The thermally unstable nitroamine, polynitro and azo compounds shown in Fig. 3 were chosen for reactions with TATOT.

2 Results and discussion

2.1 Synthesis and characterization

Compounds **1–8** and their corresponding silver or ammonium salts were prepared following the literature procedures {see (ESI)†}.[37–44] The planar 3,6,7-triamino-7*H*-[1,2,4]triazolo[4,3-b][1,2,4]triazolium (TATOT) cation was selected for molecular recognition studies with various energetic anions because of its planar geometry. The silver salts or ammonium salts of compounds **1–8** (Fig. 3) were reacted with the hydrochloride salt of 3,6,7-triamino-[1,2,4]triazolo[4,3-b][1,2,4]triazole (TATOT·HCl) in aqueous solution to obtain insensitive sandwich energetic materials **ISEMs 1–8** (Scheme 1).

In **ISEM-1**, the π–π interaction brought about by stacking of a dianion and two mono cations is visualized by plotting noncovalent interactions (NCI plots)[45,46] (Fig. 4M). Single crystals of **ISEM-2** suitable for X-ray analysis are obtained by slow evaporation from water. It crystallizes in a monoclinic ($P2_1/c$) space group with one dinitramide anion, two TATOT cations and two water molecules to give $C_{10}H_{18}N_{24}O_{10}$, with a density of 1.758 g cm^{-3} at 100 K (See ESI, Section S2†).

In **ISEM-2**, each dinitramide anion is sandwiched between TATOT cations through π-philic molecular recognition interactions (Fig. 4B and N). The eight O atoms from the two nitroamino groups are fixed by H-bonds from the surrounding TATOT cations and water molecules, with lengths ranging from 1.80 Å to 2.56 Å. Single crystals of **ISEM-3** suitable for X-ray analysis were obtained by slow evaporation from dimethyl sulfoxide. It crystallizes in a monoclinic ($P2_1/n$) space group

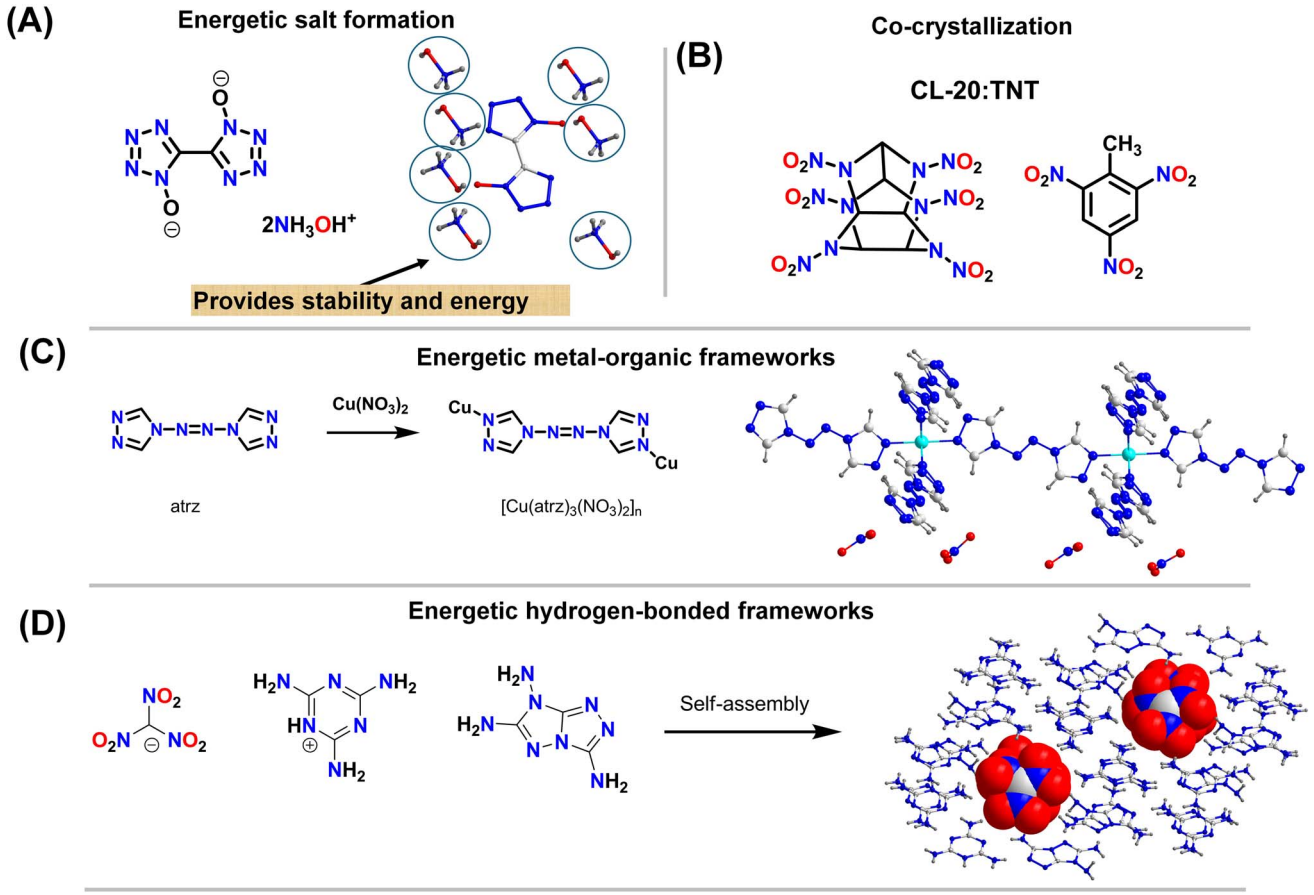

Fig. 2 Strategies to take advantage of stabilizing interactions in the production of new energetic materials. (A) Energetic salt formation. (B) Co-crystallization. (C) Energetic metal–organic frameworks. (D) Hydrogen-bonded frameworks.

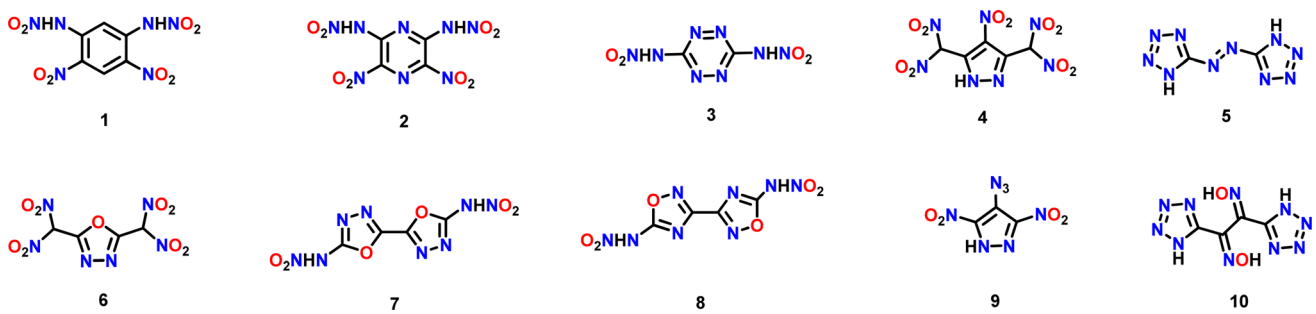

Fig. 3 Compounds chosen for this study.

with one dinitramide anion, and two TATOT cations to give $C_8H_{14}N_{24}O_4$, with a density of 1.808 g cm^{-3} at 100 K (ESI, Section S2†). In **ISEM-3**, each dinitramide anion is sandwiched between TATOT cations through π-philic molecular recognition (Fig. 4C and O). The four O atoms from two nitroamino groups are fixed by H bonds from the surrounding TATOT cations, with lengths ranging from 1.88 Å to 2.57 Å. The π–π interactions aroused by stacking of the dianion and two mono cations are visualized by plotting non-covalent interactions plots. In comparison with **ISEM-1**, the rings in **ISEM-3** are found to be more displaced.

Single crystals of **ISEM-4** and **ISEM-5** are obtained by slow evaporation from H_2O and methanol co-solvent mixtures. **ISEM-4** crystallizes in a monoclinic (*Pc*) space group to give a formula $C_{11}H_{14}N_{23}O_{10}$, with a density of 1.860 g cm^{-3} at 100 K and **ISEM-5** crystallizes in a triclinic ($P\bar{1}$) space group to give a formula $C_8H_{12}N_{26}$, with a density of 1.674 g cm^{-3} at 100 K. In both compounds, each dianion is sandwiched between TATOT cations (Fig. 4D–E, 4P and 4Q). In **ISEM-4**, the ten O atoms from five nitro groups are fixed by H bonds from the surrounding TATOT cations, with lengths ranging between 1.87 Å to 2.62 Å, In **ISEM-5**, the length of H-bonds range from 1.98 Å to 2.29 Å.

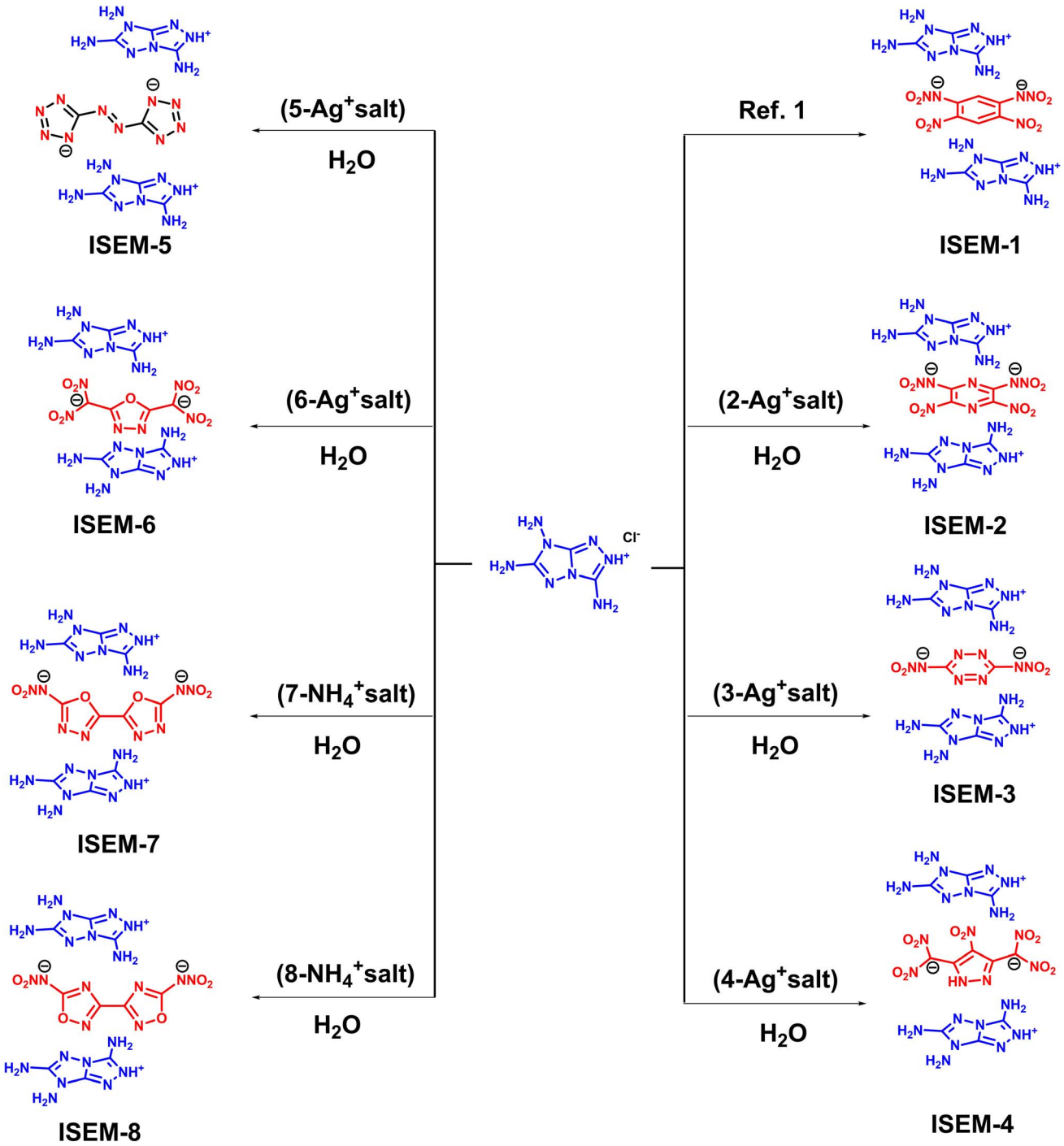

Scheme 1 Sandwiching azo, nitro, nitroamino high-energy materials with TATOT.

The length of π–π stacking interactions is found in the range of 3.35 Å to 3.37 Å. For **ISEM-6**, single crystals were also obtained by slow evaporation from H_2O and methanol co-solvent mixtures. **ISEM-6** crystallizes in an orthorhombic ($Pca2_1$) space group to give a formula $C_{10}H_{14}N_{22}O_9$, with a density of 1.855 g cm^{-3} at 100 K. The sandwich structure is shown in Fig. 4F and R.

The effect of solvent on the packing of these sandwich molecules was observed. For **ISEMs 1**, **3**, **4**, **5**, and **6** the single crystals suitable for X-ray analysis were obtained from water:methanol co-solvent mixtures. Suitable single crystals for **ISEM-2** only grew in water due to slight solubility. Similar to **ISEM-2**, single crystals for slightly water soluble **ISEM-3** and **ISEM-6** were obtained to learn if the H_2O would disrupt the π-philic molecular recognition between the rings. From H_2O, **ISEM-3** crystallizes in a monoclinic ($P2_1/n$) space group with one H_2O molecule, one dinitramide anion, and two TATOT cations to give a formula $C_8H_{14}N_{24}O_4 \cdot H_2O$ with a density of 1.759 g cm^{-3} at 100 K. It is seen that the H_2O molecule in the lattice does not disrupt the π-philic molecular recognition

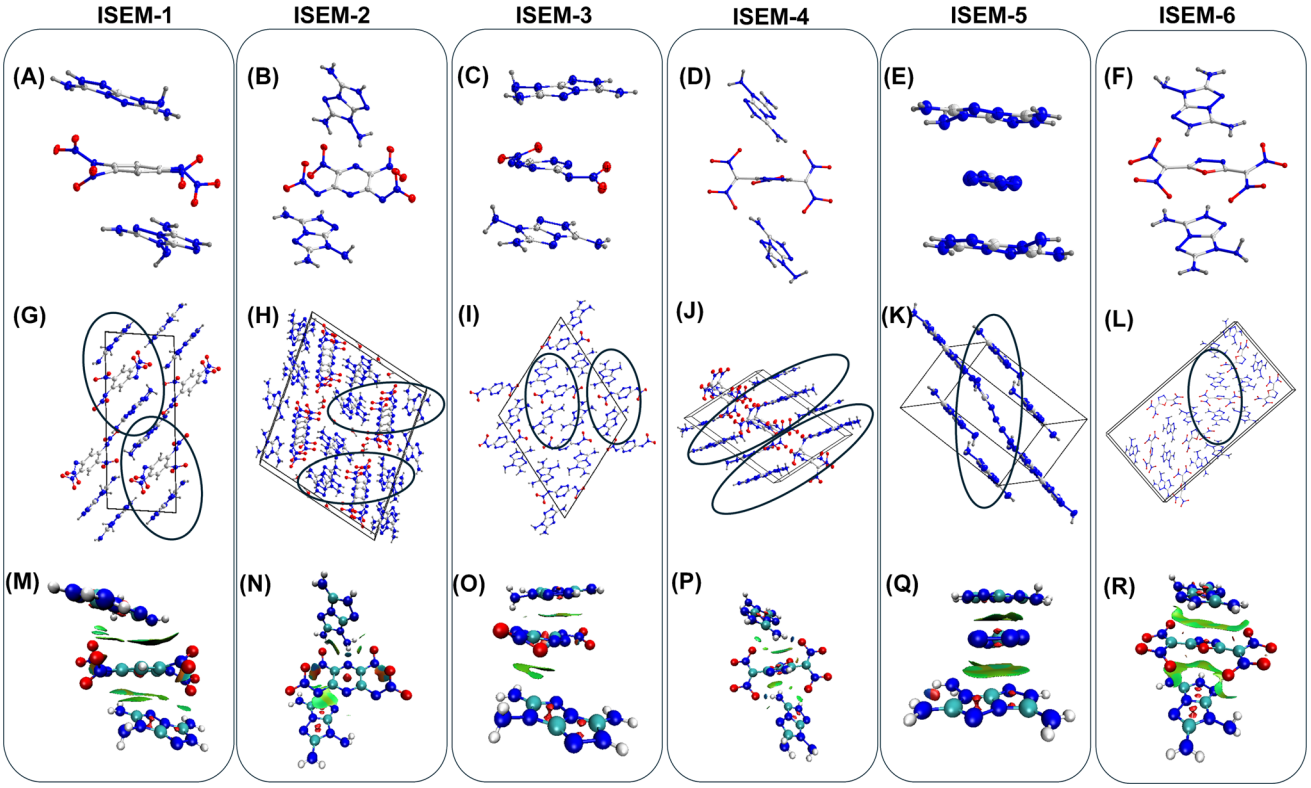

Fig. 4 Molecular structures (A) **ISEM-1** (ref. 37). (B) **ISEM-2**. (C) **ISEM-3**. (D) **ISEM-4**. (E) **ISEM-5**. (F) **ISEM-6**. Packing diagrams. (G) **ISEM-1** (ref. 37). (H) **ISEM-2**. (I) **ISEM-3**. (J) **ISEM-4**. (K) **ISEM-5**. (L) **ISEM-6**. π-Philic molecular recognition between the ring visualized through NCI plots (M) **ISEM-1**. (N) **ISEM-2**. (O) **ISEM-3**. (P) **ISEM-4**. (Q) **ISEM-5**. (R) **ISEM-6**.

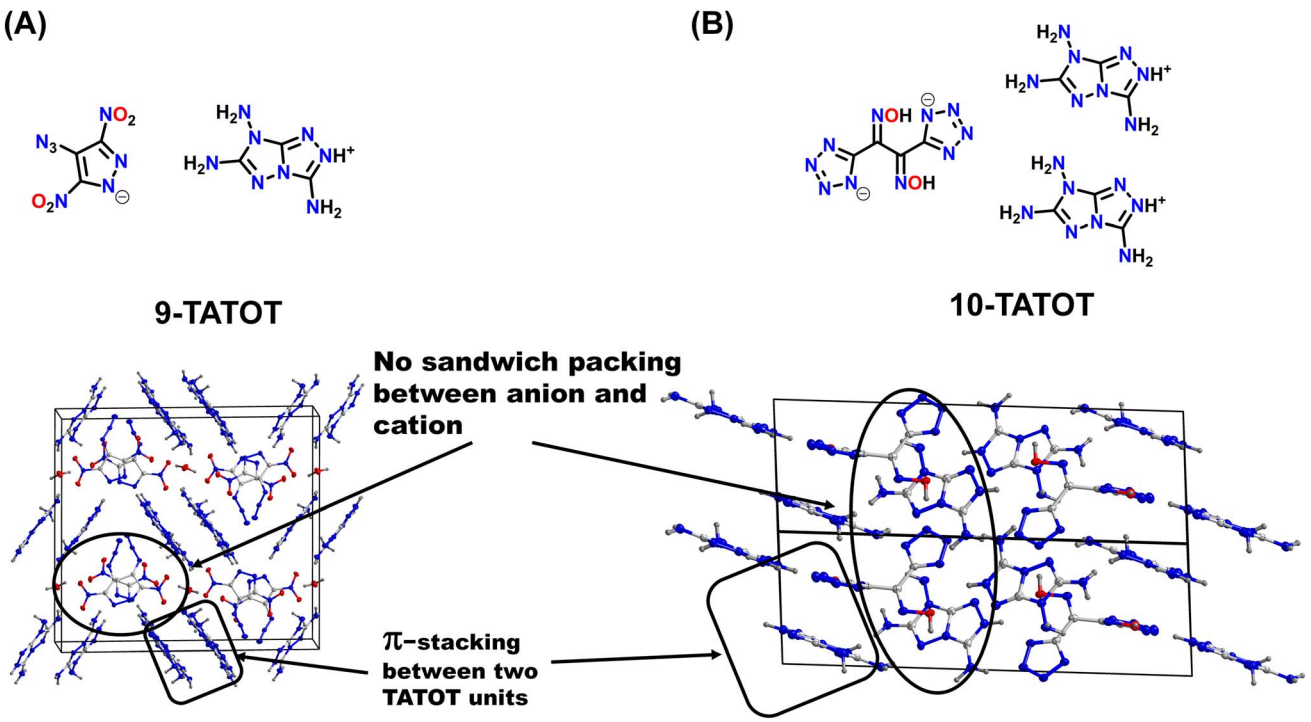

Fig. 5 Reaction of TATOT with monoanions. (A) **9-TATOT**. (B) **10-TATOT** (ref. 48).

between the rings (See ESI, Section 2†). For **ISEM-5**, the single crystals obtained from H_2O show different cell parameters. From H_2O, **ISEM-5** crystallizes in a monoclinic space group $P2_1/c$ with two molecular moieties per unit cell.[36] From H_2O, **ISEM-6** crystallizes in a monoclinic ($Pna2_1$) space group with one H_2O molecule, one dinitramide anion, and two TATOT cations to give a formula $C_{10}H_{14}N_{22}O_9 \cdot H_2O$ with a density of 1.792 g cm^{-3} at 100 K. It is seen that the H_2O molecule in the lattice slightly disrupts the π-philic molecular recognition between the rings (See ESI, Section 2†). The water:methanol co-solvent mixture is found to be the best combination to grow crystals for these sandwich molecules.

To determine the importance of π-philic molecular recognition between two TATOT cations and a planar anion ring, the reactions of a non-planar anions with TATOT were examined. The silver salt of 4-azido-3,5-dinitropyrazole[47] was reacted with TATOT. HCl in aqueous solution to obtain **9**. Since these molecules lack the π-philic molecular recognition sites between the two TATOT cations and anion, sandwich-type packing is not observed (Fig. 5A). Another such example from the literature which includes a non-planar dianion is **10-TATOT.** It also lacks the π-philic molecular recognition with TATOT due to its non-planar framework (Fig. 5B).[48]

2.2 Thermal and sensitivity properties

With a heating rate of 5 °C min^{-1}, the thermal decomposition temperatures of **ISEM-1**, **ISEM-2** and **ISEM-3** occurred at 253 °C, 189 °C, and 238 °C, respectively, which are significantly higher than their nitroamine precursors **1**, **2** and **3**, respectively (Fig. 6); decomposition of **ISEM-4** and **ISEM-5** occurred at 203 °C and

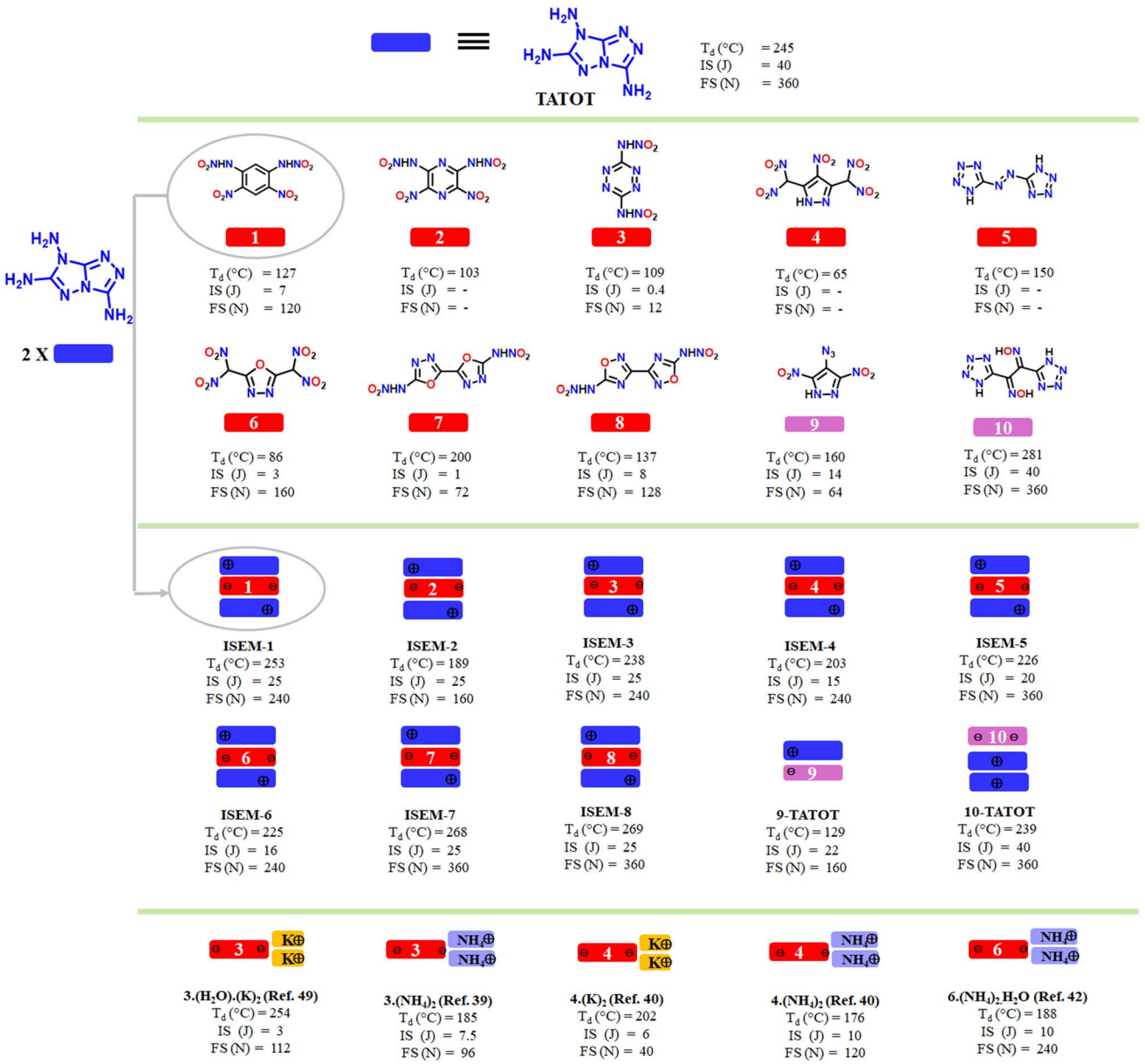

Fig. 6 Thermal and sensitivity properties.

226 °C, respectively; decomposition of **ISEMs 6–8** at 225 °C, 268 °C and 269 °C, respectively. The thermal and sensitivity properties of **ISEMs 6–8** are also compared with typical metal salts and non-metallic salts (Fig. 6) to highlight the advantages of this structure.[39,40,42,49] For compounds **9-TATOT** and **10-TATOT**, the thermal decomposition temperatures are found to be lower than those for the neutral precursors **9** and **10**, respectively (Fig. 6).

To better understand the relationship between molecular structures and their physical characteristics, Hirshfeld surfaces and 2D fingerprints were examined (Fig. 7A–F).[50,51] In **ISEMs 1–4** and **6**, a large sum of stabilizing interactions such as O–H···N and N–H···N, enhances molecular stability (Fig. 7A–D, F). In **ISEMs 1–4** and **6** the total number of O–H···N and N–H···N interactions is around 60% or above. In **ISEM-5**, a large number of N–H···N interactions (65%) contribute towards molecular stability (Fig. 7E). For **ISEMs 1–6**, the contributions of N···N, and N···C interactions which denote p–p stacking are found in the range of 7–17%.

For **ISEMs 1–8** sensitivities to impact and friction were measured by using BAM standard methods,[52,53] and are given in Fig. 6. These compounds show very low sensitivity towards impact in comparison with their neutral precursor and silver salts. The low sensitivities of compounds are further explained from both the crystal structure and at the molecular level. At the molecular level, sensitivities of materials toward impact are very

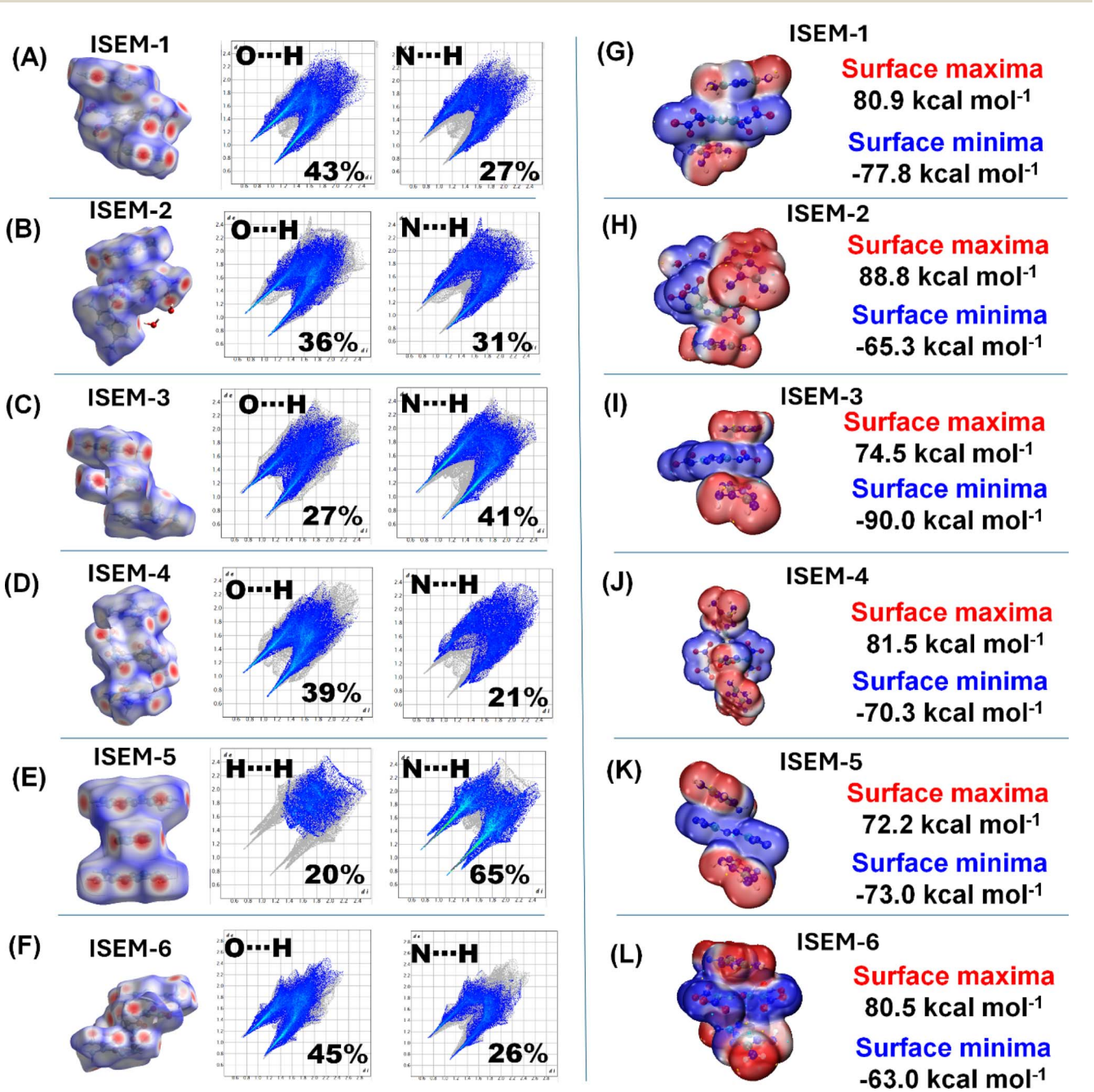

Fig. 7 (A–F) Hirshfeld surfaces and 2D fingerprint plots. (G–L) Electrostatic potential (ESP) surfaces.

Table 1 Physicochemical properties of ISEM 1–8

Compound	P^a (g cm^{-3})	$\Delta H_f{}^b$ kJmol^{-1}	P^c (GPa)	$D_v{}^d$(m s^{-1})
ISEM-1	1.76[e]	1277.9[e]	26.2	8245
ISEM-2	1.72	1381.3	26.5	8267
ISEM-3	1.75	1699.8	29.2	8752
ISEM-4	1.80	986.0	28.2	8436
ISEM-5	1.63	1811.8[f]	22.9	8054
ISEM-6	1.80	903.9	27.9	8435
ISEM-7	1.76	1313.6	26.0	8305
ISEM-8	1.75	1200.1	25.1	8185
RDX[g]	1.80	92.6	34.2	8836

[a] Density at 25 °C using gas pycnometer. [b] Molar enthalpy of formation (calculated using isodesmic reactions with the Gaussian 03 suite of programs (revision D.01)). [c] Pressure. [d] Velocity (calculated using EXPLO5 version 7.01.01). [e] Ref [37]. [f] Ref [36]. [g] Ref [56].

much related to their electrostatic surface potentials (ESPs). The electrostatic potentials (ESP) of **ISEMs 1–6** were calculated by using the B3LYP/6-311G(d, p) method with optimized structures.[45] The calculated ESPs mapped surfaces of ISEM **1–6** are shown in Fig. 7G–L. It is seen that for **ISEMs 1–6**, the positive ESP concentrates on the TATOT cation, while the negative ESP distributes on the dianion.

2.3 Detonation properties

To calculate the detonation properties, room temperature densities for **ISEMs 1–8** were measured using a gas pycnometer and are in the range of 1.63–1.80 g cm^{-3}, respectively (Table 1). The enthalpies of formation (ΔH_f) for compounds ISEMs **1–8** are given in Table 1.[54] All compounds have positive enthalpies of formation in the range of 903.9 kJ mol^{-1} and 1811.8 kJ mol^{-1}, respectively. With experimental densities and calculated enthalpies of formation, the detonation properties of compounds were calculated using EXPLO5 (v7.01.01).[55] The calculated detonation velocities are in the range of 8054–8752 m s^{-1}, and detonation pressures fall between 22.9–29.2 GPa, respectively. The detonation properties of **ISEM-3** are found to be comparable with **RDX**.

3 Conclusions

In conclusion, π-philic molecular recognition was employed to design and synthesize a new class of energetic sandwich materials. Molecular insights into structure–property relationships are provided through X-ray and theoretical studies, which highlight the role of weak but pivotal non-covalent interactions. In addition to improved thermal stability and insensitivity, these materials exhibit acceptable physiochemical properties and very low solubilities in water. We believe these insights will enable further advances toward constructing energetic sandwich materials suitable for practical applications.

Data availability

The data underlying this study are available in the published article and its online ESI.†

Conflicts of interest

The authors declare that they have no competing financial interests or personal relationships that could have influenced the work reported in this paper.

Acknowledgements

The diffractometer (Rigaku Synergy S) for SC-XRD was purchased with support from the National Science Foundation (MRI program) under grant no.1919565. We are grateful to the Fluorine-19 fund for support. MF – National Science Centre's PRELUDIUM-BIS grant no. 2020/39/O/ST5/03293; MF – Polish National Agency for Academic Exchange grant no. BPN/PRE/2022/1/00043.

References

1 K. E. Riley and P. Hobza, *Acc. Chem. Res.*, 2013, **46**, 927–936.
2 M. J. Plevin, D. L. Bryce and J. Boisbouvier, *Nat. Chem.*, 2010, **2**, 466–471.
3 A. S. Mahadevi and G. N. Sastry, *Chem. Rev.*, 2016, **116**, 2775–2825.
4 P. Kollman, *New Compr. Biochem.*, 1984, **6**, 55–71.
5 C. R. Martinez and B. L. Iverson, *Chem. Sci.*, 2012, **3**, 2191–2201.
6 G. B. McGaughey, M. Gagné and A. K. Rappé, *J. Biol. Chem.*, 1998, **273**, 15458–15463.
7 B. J. J. Timmer and T. J. Mooibroek, *J. Chem. Educ.*, 2021, **98**, 540–545.
8 G. Gil-Ramírez, D. A. Leigh and A. J. Stephens, *Angew. Chem., Int. Ed.*, 2015, **54**, 6110–6150.
9 J. Singh, H. Kim and K. W. Chi, *Chem. Rec.*, 2021, **21**, 574–593.
10 S. Shanmugaraju and P. S. Mukherjee, *Chem. Commun.*, 2015, **51**, 16014–16032.
11 D. S. Kretić, J. I. Radovanović and D. Z. Veljković, *Phys. Chem. Chem. Phys.*, 2021, **23**, 7472–7479.
12 J. Singh, R. J. Staples and J. M. Shreeve, *Sci. Adv.*, 2023, **9**, eadk375.
13 G. Liu, S. H. Wei and C. Zhang, *Cryst. Growth Des.*, 2020, **20**, 7065–7079.
14 O. Bolton and A. J. Matzger, *Angew. Chem., Int. Ed.*, 2011, **50**, 8960–8963.
15 J. Zhang, Q. Zhang, T. T. Vo, D. A. Parrish and J. M. Shreeve, *J. Am. Chem. Soc.*, 2015, **137**, 1697–1704.
16 S. Banik, P. Kumar, V. D. Ghule, S. Khanna, D. Allimuthu and S. Dharavath, *J. Mater. Chem. A*, 2022, **10**, 22803–22811.
17 T. M. Klapötke, J. Stierstorfer and A. U. Wallek, *Chem. Mater.*, 2008, **20**, 4519–4530.
18 A. A. Larin, A. N. Pivkina, I. V. Ananyev, D. V. Khakimov and L. L. Fershtat, *Front. Chem.*, 2022, **10**, 1012605.
19 P. Bhatia, K. Pandey, B. Avasthi, P. Das, V. D. Ghule and D. Kumar, *J. Org. Chem.*, 2023, **88**, 15085–15096.
20 W. Hu, J. Tang, X. Ju, Z. Yi, H. Yang, C. Xiao and G. Cheng, *ACS Cent. Sci.*, 2023, **9**, 742–747.

21 Q. Lang, Q. Sun, Q. Wang, Q. Lin and M. Lu, *J. Mater. Chem. A*, 2020, **8**, 11752–11760.
22 N. Fischer, D. Fischer, T. M. Klapötke, D. G. Piercey and J. Stierstorfer, *J. Mater. Chem.*, 2012, **22**, 20418.
23 T. M. Klapötke and M. Suceska, *Z. Anorg. Allg. Chem.*, 2021, **647**, 572–574.
24 J. Tang, H. Xiong, G. Zhang, Y. Tang, H. Yang and G. Cheng, *Chem. Commun.*, 2022, **58**, 11847–11850.
25 D. Fischer, J. Ennifer, L. Gottfried, T. M. Klapötke, K. Karaghiosoff, J. Stierstorfer and T. G. Witkowski, *Angew. Chem., Int. Ed.*, 2016, **128**, 16366–16369.
26 M. Benz, T. M. Klapötke, J. Stierstorfer and M. Voggenreiter, *ACS Appl. Eng. Mater.*, 2022, **1**, 3–6.
27 Y. Zhou, H. Gao and J. M. Shreeve, *Energ. Mater. Front.*, 2020, **1**, 2–15.
28 H. Gao and J. M. Shreeve, *Chem. Rev.*, 2011, **111**, 7377–7436.
29 T. M. Klapötke, *Chemistry of High-Energy Materials*, De Gruyter, 2022, vol. 6.
30 J. P. Agrawal, *High Energy Materials*, Wiley, 2010.
31 A. J. Bennett, L. M. Foroughi and A. J. Matzger, *J. Am. Chem. Soc.*, 2024, **146**, 1771–1775.
32 J. Zhang, Y. Feng, Y. Bo, A. K. Chinnam, J. Singh, R. J. Staples, X. He, K. Wang, J. Zhang and J. M. Shreeve, *Chem*, 2022, **8**, 2678–2687.
33 J. Zhang, Z. Zhu, M. Zhou, J. Zhang, J. P. Hooper and J. M. Shreeve, *ACS Appl. Mater. Interfaces*, 2020, **12**, 40541–40547.
34 J. Zhang, Y. Feng, R. J. Staples, J. Zhang and J. M. Shreeve, *Nat. Commun.*, 2021, **12**, 1–7.
35 V. A. Kuehl, A. M. Schmalzer, C. J. Snyder and D. E. Chavez, *ACS Omega*, 2023, **8**, 38879–38884.
36 T. M. Klapötke, P. C. Schmid, S. Schnell and J. Stierstorfer, *Chem.–Eur. J.*, 2015, **21**, 9219–9228.
37 J. Singh, S. Lal, R. J. Staples and J. M. Shreeve, *Mater. Chem. Front.*, 2022, **6**, 933–938.
38 J. Singh, A. K. Chinnam, R. J. Staples and J. M. Shreeve, *Inorg. Chem.*, 2022, **61**, 16493–16500.
39 H. Li, T. Zhang, Z. Li, Y. Wang, J. Ren and T. Zhang, *J. Energ. Mater.*, 2022, **40**, 15–33.
40 J. Singh, R. J. Staples and J. M. Shreeve, *ACS Appl. Mater. Interfaces*, 2021, **13**, 61357–61364.
41 M. M. Williams, W. S. Mcewan and R. A. Henry, *J. Phys. Chem.*, 1957, **61**, 261–267.
42 Q. Yu, P. Yin, J. Zhang, C. He, G. H. Imler, D. A. Parrish and J. M. Shreeve, *J. Am. Chem. Soc.*, 2017, **139**, 8816–8819.
43 T. S. Hermann, K. Karaghiosoff, T. M. Klapötke and J. Stierstorfer, *Chem.–Eur. J.*, 2017, **23**, 12087.
44 Y. Cao, H. Huang, X. Lin, J. Yang and X. Gong, *New J. Chem.*, 2018, **42**, 11390–11395.
45 T. Lu and F. Chen, *J. Comput. Chem.*, 2012, **33**, 580–592.
46 E. R. Johnson, S. Keinan, P. Mori-Sánchez, J. Contreras-García, A. J. Cohen and W. Yang, *J. Am. Chem. Soc.*, 2010, **132**, 6498–6506.
47 X. Y. Zhang, X. Y. Lin, B. Y. Guo, C. Tan and Y. Han, *J. Mol. Struct.*, 2022, **1267**, 133526.
48 J. Singh, R. J. Staples and J. M. Shreeve, *J. Mater. Chem. A*, 2023, **11**, 12896–12901.
49 T. Zhang, J. Du, Z. Li, X. Lin, L. Wang, L. Yang and T. Zhang, *CrystEngComm*, 2019, **21**, 765–772.
50 M. A. Spackman and J. J. McKinnon, *CrystEngComm*, 2002, **4**, 378–392.
51 M. A. Spackman and D. Jayatilaka, *CrystEngComm*, 2009, **11**, 19–32.
52 NATO, Standardization Agreement 4489 (STANAG4489), Explosives, Impact Sensitivity Tests, 1999.
53 NATO, Standardization Agreement 4487 (STANAG 4487), Explosives, Friction Sensitivity Tests, 2002.
54 M. J. Frisch, G. W. Trucks, H. B. Schlegel and G. E. Scuseria, *et al.*, *Revision D.01*, Gaussian Inc., Wallingford CT, 2003.
55 M. Sućeska, *EXPLO5, Version 6.01*, Brodarski Institute, 2019.
56 R. Mayer, J. Köhler and A. Homburg, *Explosives*, Wiley-VCH, 2007.